

# Non-equilibrium phases of Fermi gas inside a cavity with imbalanced pumping

Xiaotian Nie and Wei Zheng\*

*Hefei National Laboratory for Physical Sciences at the Microscale and Department of Modern Physics, University of Science and Technology of China, Hefei 230026, China*

*CAS Center for Excellence in Quantum Information and Quantum Physics, University of Science and Technology of China, Hefei 230026, China and*

*Hefei National Laboratory, University of Science and Technology of China, Hefei 230088, China*  
(Dated: July 17, 2023)

In this work, we investigate the non-equilibrium dynamics of one-dimensional spinless fermions loaded in a cavity with imbalanced pumping lasers. Our study is motivated by previous work on a similar setup using bosons, and we explore the unique properties of fermionic systems in this context. By considering the imbalance in the pumping, we find that the system exhibits multiple superradiant steady phases and an unstable phase. Furthermore, by making use of the hysteresis structure of superradiant phases, we propose a unidirectional topological pumping. Unlike the usual topological pumping in which the driving protocol breaks time reversal symmetry, the driving protocol can be time reversal invariant in our proposal.

## INTRODUCTION

Ultracold atomic gases coupled to optical cavities provide a versatile platform for studying quantum many-body physics. On the one hand, cavity photons mediate long-range interactions between atoms inside a cavity, which can lead to new phases of atom-cavity hybridized systems. On the other hand, the leaking of the photons from the cavity provides a dissipation channel that will drive the system away from equilibrium, exhibiting rich dynamics and providing a way to detect them. One typical setup involves atoms loaded into a cavity, which is pumped by a pair of counterpropagating pumping lasers. Usually, the intensities of the two pumping lasers are balanced, such that they form a standing wave, and create a static optical lattice for the atoms. In the past decade, significant advances have been made based on such balanced pumping setups. For example, superradiance of the cavity field has been studied and observed with bosonic [1–13][14–16] and fermionic atoms [17–25][26] inside cavities respectively. Dissipative time crystals, which can break discrete or continuous time translation symmetry [27–36], have also been predicted and observed in such systems. More on-equilibrium dynamical phases without steady states have been explored in balanced pumped cavities [37–40].

Recently, there has been growing interest in exploring the effects of imbalanced pumping lasers on atom-cavity hybridized systems. The intensities of the two counter-propagating lasers can be tuned to be unequal, such that the atoms feel both standing and travelling waves. The asymmetry in the pumping leads to the emergence of novel phases, including distinct superradiant phases and self-organized charge pumping [16, 40]. However, though most of the works are focused on the bosonic atoms inside cavities with imbalanced pumping, the behavior of fermions in this regime remains largely unexplored.

In this work, we investigate a one-dimensional cloud of spinless fermions loaded into an optical cavity and pumped by a pair of transverse laser beams of unequal intensities. We found new superradiant steady states which did not appear in the bosonic case, and predicted a self-organized dynamical phase in such systems. Based on these new superradiant phases, we design a unidirectional topological pumping. Unlike the usual topological pumping in which the driving protocol breaks time reversal symmetry, the driving protocol can be time reversal invariant in our proposal. It is the self-organization and dissipation that stabilize the quantization of the pumping. Our work provides insights into the behavior of fermions in cavity systems, and paves the way for future studies of topological phenomena inside cavities.

## THE SETUP AND MODEL

The experiment setup is shown in Fig.1, where fermionic atoms are loaded into a single-mode optical cavity, which is set along the  $y$ -axis. The electrical field of the cavity mode is  $\hat{\mathbf{E}}_c(\mathbf{r}) = \xi(\hat{a} + \hat{a}^\dagger) \cos(k_c y) \mathbf{e}_z$ , where  $\xi$  is the electric field strength of a single photon, and  $\hat{a}$  ( $\hat{a}^\dagger$ ) is the annihilating (creating) operator of the cavity photons. The atomic cloud is shined by a pair of counter-propagating pumping lasers along the  $x$ -axis. The electronic field of the pumping beams is  $\mathbf{E}(\mathbf{r}, t) = \mathbf{E}_+(\mathbf{r}, t) + \mathbf{E}_-(\mathbf{r}, t)$ , with counter-propagating plane waves  $\mathbf{E}_\pm(\mathbf{r}, t) = E_\pm \cos(\pm k_p x - \omega_p t) \mathbf{e}_z$ , where  $k_p$  is the wave vector of pumping beam with frequency  $\omega_p$ .

In such a setup, atoms feel a cavity-dependent potential,

$$V(\mathbf{r}) = V_{\text{pump}}(\mathbf{r}) + V_{\text{cavity}}(\mathbf{r}) + V_{\text{inter}}(\mathbf{r}).$$

Here  $V_{\text{pump}}(\mathbf{r}) = V_p \cos^2(k_p x)$  is the lattice generated by the pumping lasers, and  $V_p = u_s E_+ E_- / 2$  is the

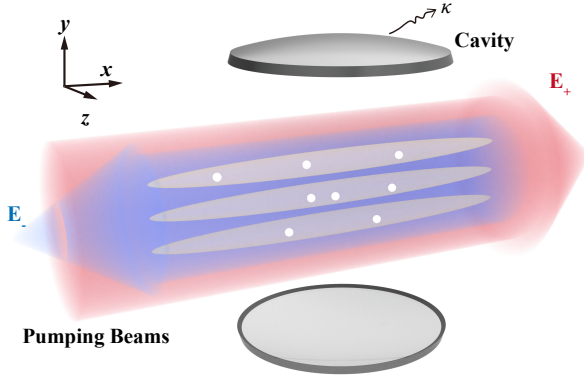


FIG. 1: A schematic illustration of spinless fermionic atoms trapped in a cavity coupled with imbalanced transverse pumping beams. The fermion atoms are restricted in a 1D tube along the pumping beams.

corresponding lattice depth.  $V_{\text{cavity}}(\mathbf{r}) = V_c \cos^2(k_c y) \hat{a}^\dagger \hat{a}$  is the lattice generated by the cavity field, and  $V_c = u_s \xi^2$  is the ac Stark shift induced by one cavity photon. The interference between the pumping beams and cavity field generates the following lattice,

$$V_{\text{inter}}(\mathbf{r}) = V_R \cos(k_p x) \cos(k_c y) (\hat{a} + \hat{a}^\dagger)/2 + V_I \sin(k_p x) \cos(k_c y) (\hat{a} - \hat{a}^\dagger)/2i,$$

where  $V_R = u_s \xi (E_+ + E_-)/2$  and  $V_I = u_s \xi (E_+ - E_-)/2$ . It describes the process of scattering a photon by atoms from pumping lasers into the cavity and vice versa. Here  $u_s$  is the scalar polarizability of the atoms. In this work, we only consider blue atomic detuning, such that  $u_s > 0$ . Note that in the case of balanced pumping,  $E_+ = E_-$ , thus  $V_I = 0$ , and atoms are only coupled to the real quadrature of the cavity. When the pumping is imbalanced  $E_+ \neq E_-$ ,  $V_I \neq 0$ , and atoms are coupled to both real and imaginary quadrature.

In this work, we further consider the motion of atoms to be restricted to the direction of propagation of the pumping beams. This can be achieved by adding extra tight trapping potentials along the  $x$  direction, such that the motion of fermions in the  $y$  and  $z$  directions is frozen, and the system is effectively one-dimensional. Therefore, the corresponding second quantized Hamiltonian is given by

$$\begin{aligned} \hat{H} = & -\Delta_c \hat{a}^\dagger \hat{a} \\ & + \int dx \hat{\psi}^\dagger(x) \left[ \frac{-\nabla^2}{2m} + V_p \cos^2(k_p x) \right] \hat{\psi}(x), \\ & + \int dx \hat{\psi}^\dagger(x) [V_R \cos(k_p x) (\hat{a} + \hat{a}^\dagger)/2] \hat{\psi}(x) \\ & + \int dx \hat{\psi}^\dagger(x) [V_I \sin(k_p x) (\hat{a} - \hat{a}^\dagger)/2i] \hat{\psi}(x) \end{aligned} \quad (1)$$

where  $\hat{\psi}(x)$  is the fermionic field operator of atoms,  $\Delta_c =$

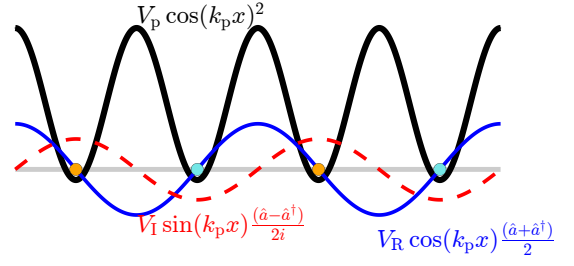


FIG. 2: Lattice potentials in the continuum. We obtain the tight binding model by only considering the  $s$ -band Wannier basis with the nearest hopping.

$\omega_p - \omega_c - NV_c$  is the effective cavity detuning and  $N$  is the total number of fermions.

In the strong pumping regime, the lattice generated by the pumping lasers is so deep, such that the Hamiltonian in the continuous space (1) can be simplified into a tight-binding (TB) model. As shown in Fig.2, the unit cell of the pumping lattice is enlarged due to the double period of the interference lattice. We denote the two orbits in one unit cell as A and B, and only consider the  $s$ -band of the pumping lattice. One obtains the tight-binding Hamiltonian as

$$\begin{aligned} \hat{H}_{\text{TB}} = & -\Delta_c \hat{a}^\dagger \hat{a} \\ & + \sum_j J_0 \left( \hat{c}_{j,B}^\dagger \hat{c}_{j,A} + \hat{c}_{j+1,A}^\dagger \hat{c}_{j,B} + h.c. \right) \\ & + \sum_j J_1 \frac{(\hat{a} + \hat{a}^\dagger)}{2} \left( -\hat{c}_{j,B}^\dagger \hat{c}_{j,A} + \hat{c}_{j+1,A}^\dagger \hat{c}_{j,B} + h.c. \right) \\ & + \sum_j J_2 \frac{(\hat{a} - \hat{a}^\dagger)}{2i} \left( \hat{c}_{j,A}^\dagger \hat{c}_{j,A} - \hat{c}_{j,B}^\dagger \hat{c}_{j,B} \right), \end{aligned} \quad (2)$$

where

$$\begin{aligned} J_0 = & \int_x w^* \left( x - \frac{\lambda_p}{4} \right) \left[ \frac{-\nabla^2}{2m} + V_p \cos^2(k_p x) \right] w \left( x + \frac{\lambda_p}{4} \right), \\ J_1 = & V_R \int_x w^* \left( x - \frac{\lambda_p}{4} \right) \cos(k_p x) w \left( x + \frac{\lambda_p}{4} \right), \\ J_2 = & V_I \int_x w^* \left( x - \frac{\lambda_p}{4} \right) \sin(k_p x) w \left( x - \frac{\lambda_p}{4} \right). \end{aligned}$$

Here  $w(x)$  is the  $s$ -band Wannier wave function in the  $s$ -band of the pumping lattice. Note that this model is a cavity-dependent Rice-Mele model. The coupling to the real quadrature of the cavity,  $(\hat{a} + \hat{a}^\dagger)/2$ , will tune the hopping ratio between intra- and inter- unit cells, while coupling to the imaginary quadrature of the cavity,  $(\hat{a} - \hat{a}^\dagger)/2i$ , will change the onsite energy of A/B sublattices. In the momentum space, the Hamiltonian can be expressed into

$$\hat{H}_{\text{TB}} = -\Delta_c \hat{a}^\dagger \hat{a} + \sum_k \hat{\Psi}_k^\dagger h(k, \hat{a}) \hat{\Psi}_k,$$

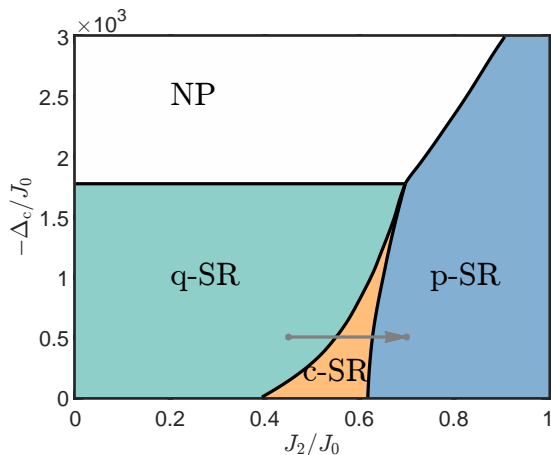


FIG. 3: Phase diagram without dissipation with  $J_1/J_0 = 0.5$ , filling  $\nu = 0.4$ . There are one normal phase (NP) and three superradiant (SR) phases. Four phases meet at a quadra-critical point. The gray path will be mentioned in Fig. 5.

where  $\hat{\Psi}_k = (\hat{c}_{k,A}, \hat{c}_{k,B})^T$  and

$$h(k, \hat{a}) = \begin{pmatrix} J_2 \text{Im}(\hat{a}) & h.c. \\ J_0(1 + e^{ik}) + J_1 \text{Re}(\hat{a})(-1 + e^{ik}) & -J_2 \text{Im}(\hat{a}) \end{pmatrix}.$$

Besides the coherent process governed by the Hamiltonian, the leaking of photons from the cavity leads to dissipative dynamics. The evolution can be described by a Lindblad quantum master equation  $\partial_t \hat{\rho} = -i [\hat{H}_{\text{TB}}, \hat{\rho}] + \kappa (2\hat{a}\hat{\rho}\hat{a}^\dagger - \{\hat{a}^\dagger\hat{a}, \hat{\rho}\})$ , where  $\kappa$  is the photon loss rate.

Apply the mean-field approximation, we obtain the self-consistent equation-of-motions of the mean cavity field,  $\alpha(t) = \langle \hat{a}(t) \rangle$ , and fermions as

$$i\partial_t \alpha(t) = (-\Delta_c - i\kappa)\alpha(t) + \langle \psi(t) | \hat{\Theta} | \psi(t) \rangle, \quad (3)$$

$$i\partial_t |\psi(t)\rangle = \hat{H}_{\text{MF}}[\alpha(t)] |\psi(t)\rangle, \quad (4)$$

where the mean field Hamiltonian of fermions,  $\hat{H}_{\text{MF}}[\alpha(t)] = \sum_k \hat{\Psi}_k^\dagger h[k, \alpha(t)] \hat{\Psi}_k$ , is dependent on the cavity field  $\alpha(t)$ , and  $\hat{\Theta}$  is given by

$$\hat{\Theta} = \frac{1}{2} \sum_k \hat{\Psi}_k^\dagger \sigma \cdot \begin{pmatrix} J_1(-1 + \cos k) \\ J_1 \sin k \\ iJ_2 \end{pmatrix} \hat{\Psi}_k.$$

By solving these equations of motion, one can obtain the dynamics of the cavity field and fermions.

### NON-DISSIPATIVE CASE

In this section, we will first explore this atom-cavity model in the non-dissipative case  $\kappa = 0$ . This will pave the way to the dissipative case.

By solving the mean-field equation-of-motions, we obtain the resulting ground state phase diagram of fixed  $J_1$

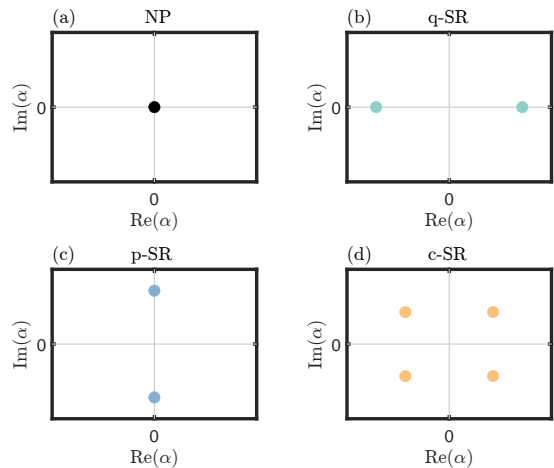


FIG. 4: Schematic configurations of  $\alpha$  of the ground states on the complex plane in four phases. NP:  $\alpha = 0$ ; q-SR: two opposite real numbers; p-SR: two opposite imaginary numbers; c-SR: four numbers in four quadrants.

shown in Fig. 3. The diagram includes one normal phase (NP) with  $\alpha = 0$  and three distinct superradiant (SR) phases  $\alpha \neq 0$ . When the photon detuning  $|\Delta_c|$  is sufficiently large, the system is in the normal phase. In the regime of small  $|\Delta_c|$  and small  $J_2$ , the system is in the q-SR phase, which stands for a superradiant phase where the cavity field  $\alpha$  is real. When  $J_2$  dominates, the system enters the p-SR phase, where  $\alpha$  is purely imaginary. Between them, there is a c-SR phase where the phase of the cavity field is not fixed, and can be tuned continuously. The four phases meet at a quadra-critical point.

The symmetry group of the Hamiltonian is product of two  $\mathbb{Z}_2$  groups,  $\{\mathcal{I}, \mathcal{T}_R\} \otimes \{\mathcal{I}, \mathcal{T}_I\} = \{\mathcal{I}, \mathcal{T}_R, \mathcal{T}_I, \mathcal{U}\}$  [41], where

$$\begin{aligned} \mathcal{T}_R &: \begin{cases} \hat{a} \rightarrow \hat{a}^\dagger \\ x \rightarrow -x \end{cases}, \\ \mathcal{T}_I &: \begin{cases} \hat{a} \rightarrow -\hat{a}^\dagger \\ x \rightarrow -x + \lambda_p/2 \end{cases}, \\ \mathcal{U} &: \begin{cases} \hat{a} \rightarrow -\hat{a} \\ x \rightarrow x + \lambda_p/2 \end{cases}. \end{aligned}$$

Note that  $\mathcal{T}_R$  represents a real-axis reflection of cavity field on the complex plane, combining with the spatial reflection of fermions.  $\mathcal{T}_I$  represents an imaginary-axis reflection with spatial reflection plus spatial translation of fermions.  $\mathcal{U} = \mathcal{T}_R \otimes \mathcal{T}_I$  is a  $\pi$ -rotation of cavity field combining a spatial translation of fermions.

We show configurations of cavity field in different phases in Fig. 4 and their symmetries in Table I. All symmetries are maintained in the NP. In SR phases, including q-SR, p-SR and c-SR phases, the  $\mathcal{U}$  symmetry is broken, but the  $\mathcal{T}_R$  or  $\mathcal{T}_I$  symmetry may survive respectively. The q-SR phase breaks the  $\mathcal{T}_I$  symmetry and keeps the  $\mathcal{T}_R$  symmetry, thus the phase of cavity is either 0 or  $\pi$ .

TABLE I: Comparison table of symmetries in different phases

| Phase | $\arg(\alpha)$ | $\mathcal{T}_R$ | $\mathcal{T}_I$ | $\mathcal{U}$ |
|-------|----------------|-----------------|-----------------|---------------|
| NP    | \              | ✓               | ✓               | ✓             |
| q-SR  | $0, \pi$       | ✓               | ×               | ×             |
| p-SR  | $\pm\pi/2$     | ×               | ✓               | ×             |
| c-SR  | Arbitrary      | ×               | ×               | ×             |

The p-SR phase is invariant under  $\mathcal{T}_I$  but breaks the  $\mathcal{T}_R$  symmetry. So the cavity phase is either  $\pi/2$  or  $-\pi/2$ . The c-SR breaks  $\mathcal{T}_R$ ,  $\mathcal{T}_I$ , and  $\mathcal{U}$  symmetries, therefore its cavity phase can be tuned continuously.

Next, we investigate the transitions between these phases. We observe that the transitions are second-order. Starting from NP, by decreasing the  $|\Delta_c/J_0|$ , the system will enter the q-SR phase. The  $\mathcal{T}_I$  symmetry is broken spontaneously as two energy minimums emerge from  $\alpha = 0$ , and then divide oppositely in real axis, but the  $\mathcal{T}_R$  symmetry is preserved. As moving further into the c-SR phase, the  $\mathcal{T}_R$  symmetry is broken by increasing  $J_2$ , and each minimum is split into complex conjugate pairs. In the c-SR phase, the order parameter  $\alpha$  changes continuously in four quadrants. Approaching the transition between the c-SR and p-SR, the upper/lower pair coalesce into a pure imaginary one respectively, and the  $\mathcal{T}_I$  symmetry is restored. Finally, the system recovers the  $\mathcal{T}_R$  symmetry by the merging of the imaginary pairs at the transition to the NP. Fig.5 shows how the phases of cavity field change continuously along the path depicted in Fig.3.

When half filling, the Fermi surface nesting arises due to the interference lattice coupling the two Fermi momenta [17–19], leading to the disappearance of the

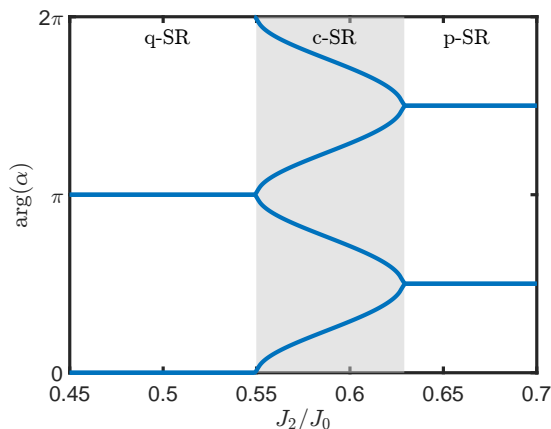


FIG. 5: The argument of  $\alpha$  changes along the gray path in Fig.3 across the c-SR phases. In the q-SR/p-SR phase, there are two steady states whose arguments are locked to  $(0, \pi)/\pm\pi/2$ . In the c-SR phase, the remaining symmetry is broken, degeneracy is doubled. The transitions are all continuous.

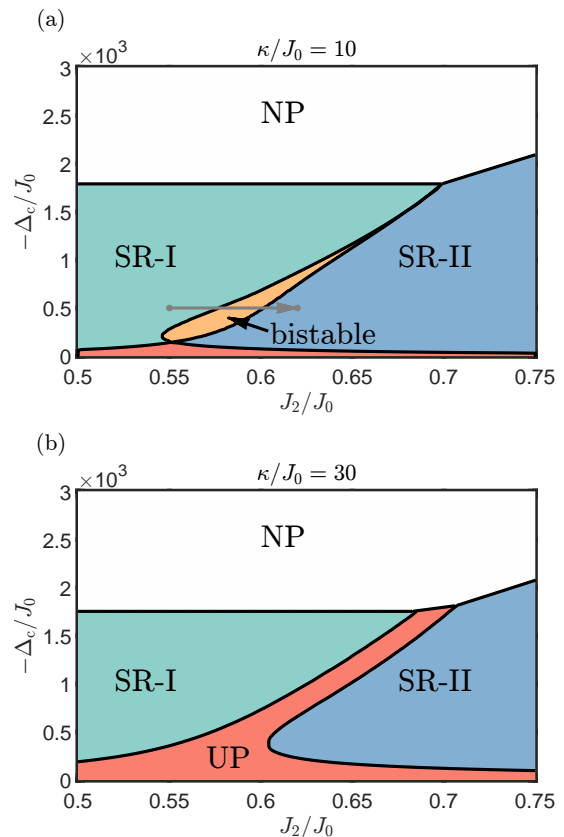


FIG. 6: The dissipative phase diagram under small and large dissipation respectively, with parameters  $J_1/J_0 = 0.5, \nu = 0.4$ . The new red region represents the unstable phase. It gradually replaces the bistable regime as  $\kappa$  increases. The gray path will be mentioned in Fig.8.

NP. In the q-SR phase, where  $\alpha$  is real, the mean-field Hamiltonian can be simplified to a Su-Schrieffer-Heeger (SSH) model [23][23–25], which has two topologically distinct phases characterized by the quantized Wannier center [42–44].

## DISSIPATIVE CASE

In this section, we will consider the fate of these phases in the presence of dissipation,  $\kappa \neq 0$ . In this situation, we numerically solve the equations of motion, and consider its long-time dynamics to seek the steady states. The phase diagram in the presence of dissipation is plotted in Fig.6. In the small  $\kappa$  regime, there exist five different regimes: a steady NP and two steady SR phases, which we denote as SR-I and SR-II. The SR-I phase is reminiscent of the q-SR phase. However, the phase of the cavity is not locked at 0 and  $\pi$ , instead it has a phase shift  $\phi_\kappa = \tan^{-1}(\frac{\Delta_c}{\kappa})$  relative to the q-SR phase. Similarly, The SR-II phase is reminiscent of the p-SR phase, but with a phase shift  $\phi_\kappa$ . In the limit  $\kappa \rightarrow 0$ , the SR-I and SR-II phases will continuously crossover to the q-

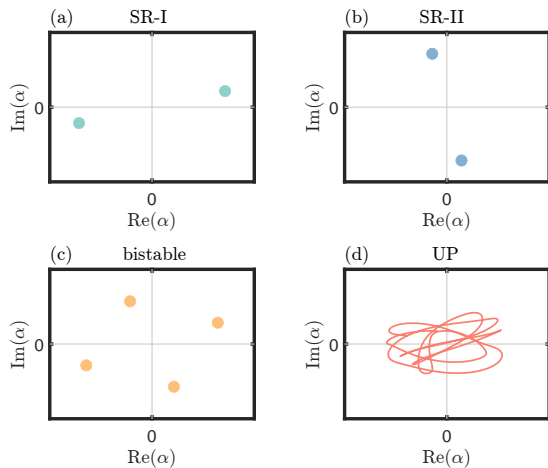


FIG. 7: Schematic configurations of  $\alpha$  of the steady states on the complex plane in SR phases, and the last figure demonstrates the trajectory of evolution in the unstable phase.

SR and p-SR phases. From the symmetry point of view, we note that both the  $\mathcal{T}_R$  and  $\mathcal{T}_I$  symmetries are absent in the presence of dissipation. This can be seen from the Lindblad quantum master equation. The only symmetry survived in the presence of dissipation is the  $\mathcal{U}$  symmetry. Thus, there are no q-SR and p-SR phases in the dissipative case. Between SR-I and SR-II phases, there is a bistable regime, in which both SR-I and SR-II phases are the steady state of the system. Whether the system stays in SR-I or SR-II state, depends on the initial condition. This bistable regime is reminiscent of the c-SR phase in the non-dissipative limit. When  $|\Delta_c|$  is small, there is an unstable phase, which does not exist in the non-dissipative case. In this phase, the system will not reach a steady state. The dissipation will drive both the cavity field and fermions to evolve incessantly. The unstable phase has already been observed in bosonic gases coupled with an imbalanced pumped cavity. In the bosonic case, since there is no bistable regime, the unstable region emerges directly from the first-order transition between the two superradiant phases as  $\kappa > 0$  [16, 40]. Here with fermions inside an imbalanced pumped cavity, As  $\kappa$  increases, we observe that the unstable region gradually squeezes the bistable regime, eventually replacing it when  $\kappa$  becomes sufficiently large, see Fig.9.

Phase transitions are also strongly influenced by dissipation. In contrast with the second-order transition in the non-dissipative case,  $\alpha$  now switches discontinuously when across the bistable regime, and exhibits a hysteresis structure. When we slowly ramp  $J_2$  up slowly from the SR-I, the system will move continuously into the bistable regime, and will suddenly jump to the SR-II phase at the right boundary. Conversely, if the system is initially prepared in the SR-II phase, then the jump will take place on the left boundary when  $J_2$  is ramped down.

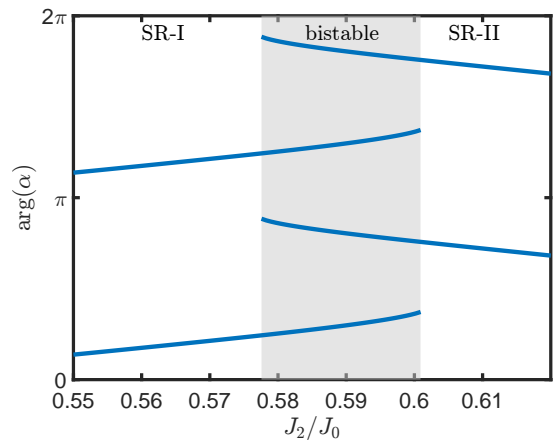


FIG. 8: The argument of  $\alpha$  changes along the gray path in Fig.6 across the bistable regime. The continuous phase transitions turn into a hysteresis.

### DISSIPATION INDUCED UNIDIRECTIONAL TOPOLOGICAL PUMPING

It has been shown by Thouless that when parameters of a 1D insulator, are driven adiabatically to complete a cycle, the charge pumped through the bulk is quantized [25, 45, 46]. To pump nonzero quantized charges, the way of the external driving should break the time reversal symmetry (TRS). For example, the driving protocol could be chosen as  $J_1(t) = J_1 \cos(\Omega t)$  and  $J_2(t) = J_2 \sin(\Omega t)$ . Here, we employ the phase structure of these superradiance states to realize a unidirectional topological pumping by a TRS-preserved driving protocol.

The numerical results are presented in Fig.12. We perform the adiabatic driving  $J_2(t) = J_2 + \delta J_2 \cos(\Omega t)$ , such that the instantaneous steady state across the bistable

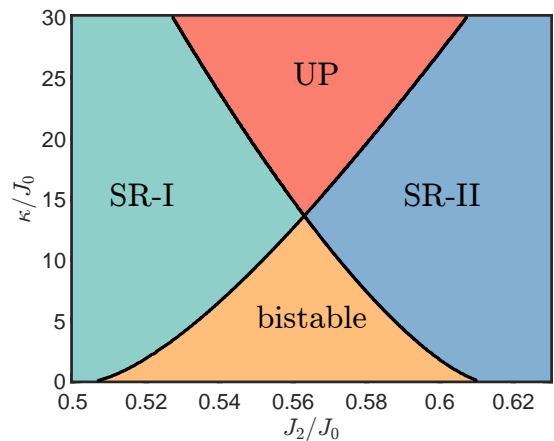


FIG. 9: A cross-section of the former phase diagrams with fixed  $\Delta_c = -300J_0$  but different  $\kappa$ . The dissipation first reduces the width of the bistable regime to zero and then brings about an unstable phase.

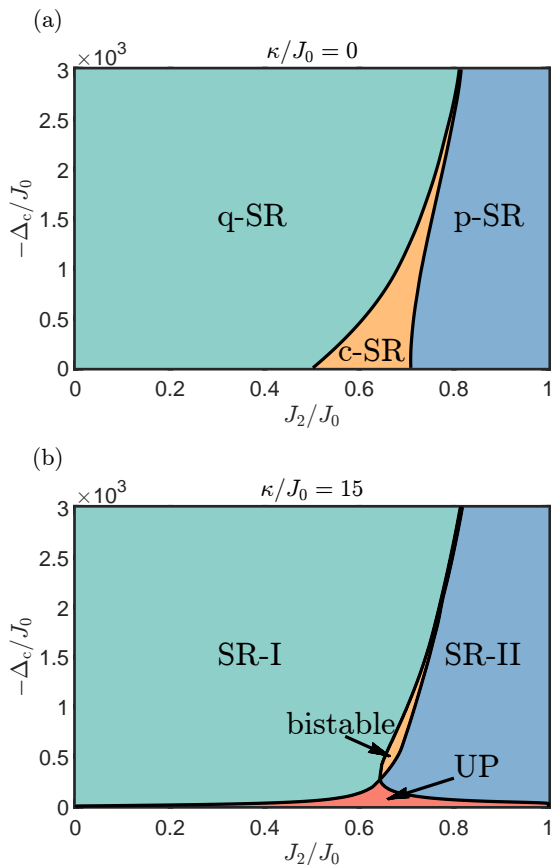


FIG. 10: Phase diagrams when half filling  $\nu = 0.5$ . The NP is unfavored due to the Fermi surface nesting.

regime with a fixed value of  $\Delta_c$ . Our simulations reveal that the evolution of the cavity field  $\alpha(t)$  forms a full circle enclosing the origin on the complex plane within a doubled period  $2T$ . That indicates this driven system exhibits a discrete time crystalline order. In addition, we observe quantized pumping in the Wannier center trajectory through time evolution [47], see Fig.12.(b).

The physics process under driving is as follows: Starting the driving from the SR-I phase, the cavity phase is close to 0, when adiabatic increasing  $J_2$ , the system will self-organized follow the driving to enter the bistable regime smoothly, and stay at one of the stable states. When  $J_2$  reaches the boundary of the bistable regime, the bistability vanishes, and the system is forced to jump to the SR-II phase. The excitation energy in this jump process can be dissipated by the loss of cavity photons, and the system will catch the SR-II steady state in a short time. In this regime, the system will again self-organized follow the driving, and the cavity phase is driven close to  $\pi/2$ . After half a period,  $J_2$  will decrease, and the system will again enter the bistable regime adiabatically, staying at an alternative stable state. When  $J_2$  is small, the system will jump to an SR-I state with cavity phase  $\alpha$  close to  $\pi$ . Repeat the driving for another period, the

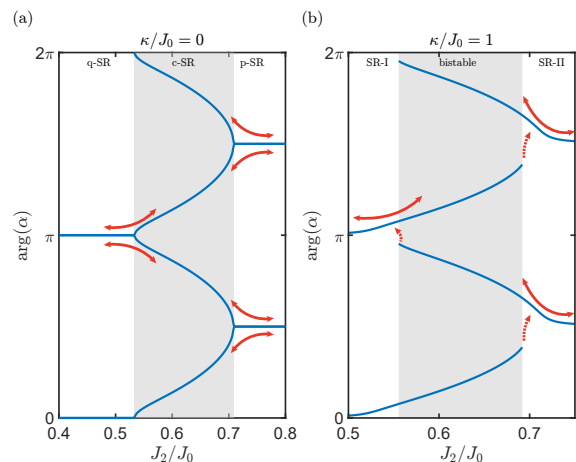


FIG. 11: The argument of  $\alpha$  across the c-SR phase or bistable regime in the non-dissipative(a) and dissipative(b) case, whose structure looks like a ladder. The dissipation can turn the bi-directional ladder into a unidirectional one.

cavity field will go back to form a cycle on the complex plane. In this process, one particle is pumped through the bulk.

We also simulate the same driving protocol without dissipation,  $\kappa = 0$ . The results are shown in Fig.12. Note that driving the parameter adiabatically between the q-SR and p-SR phases causes the cavity field  $\alpha$  to change slowly, resulting in a quantized displacement of the Wannier center during the evolution. However, the direction of the displacement is not controllable due to the spontaneous symmetry breaking at the transitions to the c-SR phase, as shown in Fig.11(a). At the phase boundaries, the phase of  $\alpha$  may increase or decrease, leading to a random back-and-forth displacement of the Wannier center over long timescales. For a long-time average, the mean displacement is zero.

Compared to the non-dissipative case, we conclude that the dissipation plays a dual role. Firstly, the presence of dissipation changes the continuous phase transitions into a bistable hysteresis structure, preventing charge pumping in both directions. Secondly, it attracts the system towards a closer steady state while losing stability, which contributes to the unidirectional motion. This direction of the pumping cannot be reversed by reversing the driving cycle since the driving protocol preserved the TRS, but it is the dissipation that breaks the TRS.

## SUMMARY

In summary, we have investigated the behavior of spinless fermions loaded into an optical cavity and pumped with transverse beams of unequal intensities. We have

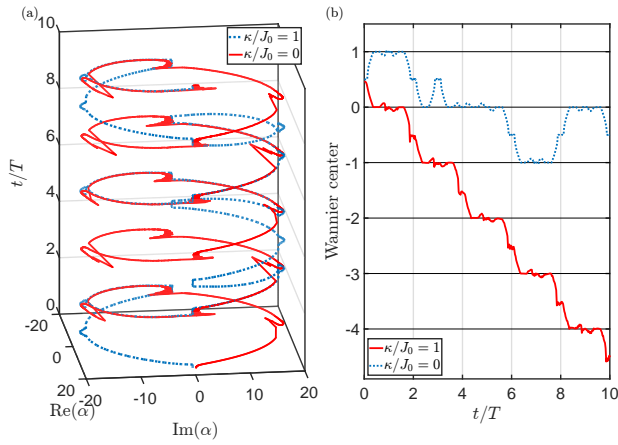


FIG. 12: The numerical results of time evolution in topological pumping, where  $J_2/J_0 = 0.625 - 0.125 \cos(\frac{2\pi}{T})$  with the period  $T = 2000\pi/J_0$ . (a) and (b) show the time evolution of the absolute value and argument of  $\alpha$ , we can see its argument keeps increasing at a long time scale. And the breaking of the discrete time translation symmetry can be seen clearly. (c) shows the trajectory of  $\alpha$  on the complex plane, it forms a circle around the origin, and has four discontinuous jumps across the axes. The Wannier center flow in (d) manifests the topological pumping directly.

observed the emergence of new superradiant phases, and a novel phenomenon called unidirectional topological pumping.

The study of cavity-coupled ultracold atomic systems continues to be a rich and exciting field of research, with many intriguing phenomena waiting to be discovered. We hope that our work will inspire further investigation into the behavior of these systems and will contribute to the ongoing effort to understand the behavior of many-body systems far from equilibrium.

*Acknowledgements.* This research is supported by the Innovation Program for Quantum Science and Technology (Grant No. 2021ZD0302000).

\* Electronic address: [zw8796@ustc.edu.cn](mailto:zw8796@ustc.edu.cn)

- [1] R. H. Dicke, *Phys. Rev.* **93**, 99 (1954).
- [2] Y. K. Wang and F. T. Hioe, *Phys. Rev. A* **7**, 831 (1973).
- [3] K. Hepp and E. H. Lieb, *Annals of Physics* **76**, 360 (1973).
- [4] P. Domokos and H. Ritsch, *Phys. Rev. Lett.* **89**, 253003 (2002).
- [5] J. K. Asbóth, P. Domokos, H. Ritsch, and A. Vukics, *Phys. Rev. A* **72**, 053417 (2005).
- [6] F. Dimer, B. Estienne, A. S. Parkins, and H. J. Carmichael, *Phys. Rev. A* **75**, 013804 (2007).
- [7] D. Nagy, G. Szirmai, and P. Domokos, *Eur. Phys. J. D* **48**, 127 (2008).
- [8] E. G. D. Torre, S. Diehl, M. D. Lukin, S. Sachdev, and P. Strack, *Phys. Rev. A* **87**, 023831 (2013).
- [9] A. Baksic and C. Ciuti, *Phys. Rev. Lett.* **112**, 173601 (2014).
- [10] L. M. Sieberer, M. Buchhold, and S. Diehl, *Rep. Prog. Phys.* **79**, 096001 (2016).
- [11] J. Larson and E. K. Irish, *J. Phys. A: Math. Theor.* **50**, 174002 (2017).
- [12] M. Soriente, T. Donner, R. Chitra, and O. Zilberberg, *Phys. Rev. Lett.* **120**, 183603 (2018).
- [13] J. Fan, G. Chen, and S. Jia, *Phys. Rev. A* **101**, 063627 (2020).
- [14] K. Baumann, C. Guerlin, F. Brennecke, and T. Esslinger, *Nature* **464**, 1301 (2010).
- [15] J. Klinder, H. Keßler, M. Wolke, L. Mathey, and A. Hemmerich, *Proc. Natl. Acad. Sci. U.S.A.* **112**, 3290 (2015).
- [16] X. Li, D. Dreon, P. Zupancic, A. Baumgärtner, A. Morales, W. Zheng, N. R. Cooper, T. Donner, and T. Esslinger, *Phys. Rev. Research* **3**, L012024 (2021).
- [17] Y. Chen, Z. Yu, and H. Zhai, *Phys. Rev. Lett.* **112**, 143004 (2014).
- [18] J. Keeling, M. J. Bhaseen, and B. D. Simons, *Phys. Rev. Lett.* **112**, 143002 (2014).
- [19] F. Piazza and P. Strack, *Phys. Rev. Lett.* **112**, 143003 (2014).
- [20] Y. Chen, H. Zhai, and Z. Yu, *Phys. Rev. A* **91**, 021602 (2015).
- [21] C. Kollath, A. Sheikhan, S. Wolff, and F. Brennecke, *Phys. Rev. Lett.* **116**, 060401 (2016).
- [22] A. Sheikhan, F. Brennecke, and C. Kollath, *Phys. Rev. A* **94**, 061603 (2016).
- [23] F. Mivehvar, H. Ritsch, and F. Piazza, *Phys. Rev. Lett.* **118**, 073602 (2017).
- [24] D. Yu, J.-S. Pan, X.-J. Liu, W. Zhang, and W. Yi, *Front. Phys.* **13**, 136701 (2018).
- [25] E. Colella, S. Ostermann, W. Niedenzu, F. Mivehvar, and H. Ritsch, *New J. Phys.* **21**, 043019 (2019).
- [26] X. Zhang, Y. Chen, Z. Wu, J. Wang, J. Fan, S. Deng, and H. Wu, *Science* **373**, 1359 (2021).
- [27] M. J. Bhaseen, J. Mayoh, B. D. Simons, and J. Keeling, *Phys. Rev. A* **85**, 013817 (2012).
- [28] F. Piazza and H. Ritsch, *Phys. Rev. Lett.* **115**, 163601 (2015).
- [29] W. Zheng and N. R. Cooper, *Phys. Rev. Lett.* **117**, 175302 (2016).
- [30] P. Kirton and J. Keeling, *New J. Phys.* **20**, 015009 (2018).
- [31] H. Keßler, J. G. Cosme, M. Hemmerling, L. Mathey, and A. Hemmerich, *Phys. Rev. A* **99**, 053605 (2019).
- [32] E. I. R. Chiacchio and A. Nunnenkamp, *Phys. Rev. Lett.* **122**, 193605 (2019).
- [33] B. Buča and D. Jaksch, *Phys. Rev. Lett.* **123**, 260401 (2019).
- [34] R. J. L. Tuquero, J. Skulte, L. Mathey, and J. G. Cosme, *Phys. Rev. A* **105**, 043311 (2022).
- [35] Z. Zhang, D. Dreon, T. Esslinger, D. Jaksch, B. Buča, and T. Donner, “Tunable non-equilibrium phase transitions between spatial and temporal order through dissipation,” (2022), [arxiv:2205.01461](https://arxiv.org/abs/2205.01461).
- [36] X. Nie and W. Zheng, *Phys. Rev. A* **107**, 033311 (2023).
- [37] P. Zupancic, D. Dreon, X. Li, A. Baumgärtner, A. Morales, W. Zheng, N. R. Cooper, T. Esslinger, and T. Donner, *Phys. Rev. Lett.* **123**, 233601 (2019).
- [38] N. Dogra, M. Landini, K. Kroeger, L. Hruby, T. Donner, and T. Esslinger, *Science* **366**, 1496 (2019).
- [39] P. Kongkhambut, J. Skulte, L. Mathey, J. G. Cosme, A. Hemmerich, and H. Keßler, *Science* **377**, 670 (2022).
- [40] D. Dreon, A. Baumgärtner, X. Li, S. Hertlein,

- T. Esslinger, and T. Donner, *Nature* **608**, 494 (2022).
- [41] P. Nataf, A. Baksic, and C. Ciuti, *Phys. Rev. A* **86**, 013832 (2012).
- [42] D. Vanderbilt and R. D. King-Smith, *Phys. Rev. B* **48**, 4442 (1993).
- [43] R. Resta, *Rev. Mod. Phys.* **66**, 899 (1994).
- [44] D. Xiao, M.-C. Chang, and Q. Niu, *Rev. Mod. Phys.* **82**, 1959 (2010).
- [45] D. J. Thouless, *Phys. Rev. B* **27**, 6083 (1983).
- [46] R. Citro and M. Aidelsburger, *Nat Rev Phys* **5**, 87 (2023).
- [47] S. Nakajima, T. Tomita, S. Taie, T. Ichinose, H. Ozawa, L. Wang, M. Troyer, and Y. Takahashi, *Nature Phys* **12**, 296 (2016).